

Coupling between electrolysis and liquid-liquid extraction in an undivided electrochemical reactor applied to the oxidation of Ce^{3+} to Ce^{4+} in an emulsion

Part II. Cell modelling*

D. HORBEZ

Rhône-Poulenc – Centre de Recherches d'Aubervilliers, 52, rue de la Haie Coq, 93308 Aubervilliers, France

A. STORCK

Laboratoire des Sciences du Génie Chimique, CNRS-ENSIC, 1, rue Grandville, BP451, 54001 Nancy, France

Received 5 March 1991; revised 13 March 1991

A model is presented which is able to predict the transient behaviour of a batch undivided electrochemical reactor with simultaneous *in situ* extraction of the product by an organic phase. The model is based on electrochemical and physical kinetic laws including mass transfer limitations for both anodic and cathodic processes and for the extraction step, mass balance equations in the aqueous and organic phases for the different species involved and a charge balance equation. With the specific example of the $\text{Ce}^{3+}/\text{Ce}^{4+}$ system, which was investigated experimentally in Part I of this work, the validity of this model is proved by comparison between the calculated time-variations of different parameters (cerium concentrations, anodic current density, partition coefficient of Ce^{4+} between the two phases) and the experimental results obtained under potentiostatic control.

| Nomenclature | | | |
|-------------------|--|-----------|--|
| | | i_{c1} | cathodic current density associated with the reduction of Ce^{4+} (A m^{-2}) |
| A_e | electrode area (m^2) | i_{c2} | cathodic current density associated with the reduction of H^+ (A m^{-2}) |
| $A(E_a), A'(E_c)$ | expressions defined in Equations 14 and 15 | i^* | dimensionless current density (expressed with respect to the anodic limiting current density at $t = 0$) |
| a, b | coefficients of the Tafel law (Equation 16) | K | equilibrium constant for the second acidity of H_2SO_4 (Equation 11) |
| a_c | specific electrode area expressed with respect to the continuous phase (m^{-1}) | K_m | equilibrium constant for the extraction mechanism (Equation 8) ($\text{mol}^2 \text{m}^{-6}$) |
| B | dimensionless parameter defined in Equation 6 | k | $= \varepsilon/(1 - \varepsilon)$ |
| C | concentration (mol m^{-3}) | k_0^0 | standard electrochemical rate constant of the $\text{Ce}^{3+}/\text{Ce}^{4+}$ system (m s^{-1}) |
| C^* | dimensionless concentration (expressed with respect to C_{30}) | k_d | mass transfer coefficient (m s^{-1}) |
| C_4^c | concentration of Ce^{4+} in the aqueous phase in equilibrium with the organic phase (mol m^{-3}) | k_{La} | overall liquid-liquid mass transfer coefficient (s^{-1}) |
| \bar{C}_4 | concentration of Ce^{4+} in the organic phase (mol m^{-3}) | m | partition coefficient of tetravalent cerium |
| D | molecular diffusion coefficient ($\text{m}^2 \text{s}^{-1}$) | R | perfect gas constant ($\text{J mol}^{-1} \text{K}^{-1}$) |
| E | electrode potential (V) | $R\gamma$ | defined in Equation 11 |
| E_0^0 | standard potential of the $\text{Ce}^{3+}/\text{Ce}^{4+}$ redox system (V) | r | $= A_{ec}/A_{ea}$ |
| F | Faraday constant ($96485 \text{ A s mol}^{-1}$) | t | time (s) |
| I | current intensity (A) | t^* | dimensionless time (defined in Equation 4) |
| i_a | anodic current density (A m^{-2}) | T | temperature (K) |
| i_{aL} | limiting anodic current density (A m^{-2}) | V | reactor volume (m^3) |

* This paper is dedicated to Professor Dr Fritz Beck on the occasion of his 60th birthday.

Greek symbols

| | |
|-------------------|---|
| α | anodic charge transfer coefficient |
| β | cathodic charge transfer coefficient |
| γ, γ' | parameters defined in Equation 6 |
| ε | volumic organic phase ratio in the dispersion |
| ν_e | number of electrons involved in the electrochemical process |
| Δt^* | time increment |

Subscripts

| | |
|---|--------------------|
| a | anodic |
| c | cathodic |
| 3 | trivalent cerium |
| 4 | tetravalent cerium |
| 0 | at time $t = 0$ |

Chemical compounds

| | |
|----------------|--------------------------------|
| $D_2EHPA = HA$ | di-2 ethylhexylphosphoric acid |
| $(HA)_2$ | dimeric form of D_2EHPA |

1. Introduction

The first part of this study [1] presented the results of an experimental analysis of the behaviour of an undivided batch electrochemical reactor with regards to the oxidation of Ce^{3+} to Ce^{4+} , extracted *in situ* by a dispersed phase of di-2 ethylhexylphosphoric acid in kerosene.

The effect of several important parameters (initial concentration of Ce^{3+} , composition and volume percentage of the organic phase, electrode potential, etc) on the performance (conversion and extraction factors of Ce^{3+} , current efficiency) of a reactor operated potentiostatically was investigated.

The simulation of the corresponding batch process based on mass and charge balances, adequate kinetic laws and mechanisms of liquid-liquid extraction of Ce^{4+} is the subject of the present second part of the paper.

2. Development of the model

The model is based on the following assumptions:

- the only reaction occurring at the anode is the oxidation of Ce^{3+} (no oxygen evolution);
- two reactions occur at the cathode: the reduction of Ce^{4+} and hydrogen evolution;
- electrochemical kinetics can be described by simple Butler-Volmer laws for the Ce^{3+}/Ce^{4+} system (see discussion in Part I), whereas a classical Tafel law holds for hydrogen evolution;
- the extraction step is selective with respect to Ce^{4+} and Ce^{3+} is not fixed by the organic phase. The mechanism of extraction developed in Part I of this work is assumed to be valid.

Under these assumptions, the development of the model is standard (see, for example, [2], [3] and [4] which report good reviews in cell modelling) and is based on mass balance equations for the different species involved in both phases taking into account electrochemical and physical kinetic laws and an overall charge balance equation.

2.1. Mass balance equations

Given the number of species and phases involved, five mass balance equations have to be considered: three for cerium present in two phases with two degrees of

oxidation, one for H^+ and one for the extraction agent (D_2EHPA).

2.1.1. Overall mass balance equation for cerium. At any time the total amount of cerium remains constant and equal to its initial value. Thus,

$$(1 - \varepsilon)VC_3 + (1 - \varepsilon)VC_4 + \varepsilon V\bar{C}_4 = (1 - \varepsilon)VC_{30} \quad (1)$$

or in dimensionless form by expressing the concentrations with respect to C_{30}

$$C_3^* + C_4^* + k\bar{C}_4^* = 1 \quad (2)$$

with $k = \varepsilon/(1 - \varepsilon)$.

2.1.2. Mass balance equation for Ce^{3+} in the aqueous phase. This may be written

$$(1 - \varepsilon)V \frac{dC_3}{dt} + \frac{i_a A_{ea}}{\nu_e F} = \frac{i_{cl} A_{cc}}{\nu_e F} \quad (3)$$

The three terms of this equation correspond, respectively, to the accumulation flux, consumption flux at the anode and production flux at the cathode (i_{cl} is the cathodic current density associated with the reduction of Ce^{4+}).

In dimensionless form Equation 3 becomes

$$\frac{dC_3^*}{dt^*} + i_a^* = r i_{cl}^* \quad (4)$$

with $r = A_{cc}/A_{ea}$, $i_a^* = i_a/(i_{aL})_0$ and $i_{cl}^* = i_{cl}/(i_{aL})_0$. The term $(i_{aL})_0$ = anodic limiting current density corresponding to the initial Ce^{3+} concentration at $t = 0$.

Hence,

$$= \nu_e F C_{30} k_{da} \frac{D_3}{D_4}$$

with $k_{da} = D_4/\delta_a$, and t^* is a dimensionless time defined by

$$t^* = t \left(k_{da} \frac{D_3}{D_4} a_{ea} \right)$$

2.1.3. Mass balance equation for Ce^{4+} in the aqueous phase. This may be written

$$(1 - \varepsilon)V \frac{dC_4}{dt} + k_L a V (1 - \varepsilon)(C_4 - C_4^e) + \frac{i_{cl} A_{cc}}{\nu_e F} = \frac{i_a A_{ea}}{\nu_e F} \quad (5)$$

The second term on the left handside corresponds to the flux of Ce^{4+} ions extracted by the organic phase; from a kinetic point of view, this flux is directly proportional to the overall liquid/liquid mass transfer coefficient k_{La} and to the driving force $(C_4 - C_4^c)$, where C_4^c is the aqueous phase concentration in equilibrium with the organic phase: $C_4^c = \bar{C}_4/m$ (m is the Ce^{4+} partition coefficient).

Introducing the dimensionless parameter

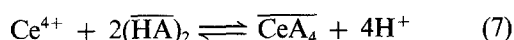
$$B = \frac{k_{La}}{k_{da}(D_3/D_4)a_{ca}} = \frac{\text{extraction rate constant}}{\text{diffusional rate constant}}$$

and expression \bar{C}_4^* from Equation 2, then Equation 5 takes the form

$$\frac{dC_4^*}{dt^*} + \gamma C_4^* + \gamma' C_3^* - \gamma' + ri_{cl}^* = i_a^* \quad (6)$$

with $\gamma = B(1 + 1/mk)$ and $\gamma' = B/mk$.

2.1.4. Mass balance equation for the extraction agent (D_2EHPA) = (HA) . In the first part of this work, it was shown that a simplified mechanism for liquid-liquid extraction was given by



where a dimer form of D_2EHPA = HA denoted $(HA)_2$ was involved.

The equilibrium constant K_m depending on the concentration of the extraction solvent (due to the fact that Equation 7 is only a simplified mechanism) is given by

$$K_m = \frac{(\overline{CeA}_4)(H^+)^4}{(Ce^{4+})(\overline{HA})_2^2} = m \frac{(H^+)^4}{(\overline{HA})_2^2} \quad (8)$$

where m is the partition coefficient of Ce^{4+} .

From Reaction 7, it follows that the mass balance for the extraction agent may be written

$$(\overline{HA})_2 = \frac{(HA)_0}{2} - 2\bar{C}_4$$

or (taking Equation 2 into account)

$$(\overline{HA})_2 = \frac{(HA)_0}{2} - 2 \frac{C_{A0}}{k} (1 - C_3^* - C_4^*) \quad (9)$$

2.1.5. Mass balance equation for H^+ . The mass balance must take into account both species H^+ and HSO_4^- . Thus,

$$(H^+) + (HSO_4^-) = 2(H_2SO_4)_0 - \frac{1}{(1 - \varepsilon)V} \times \int_0^t \frac{A_{ec} i_{e2}(t)}{F} dt + 4k\bar{C}_4 \quad (10)$$

In Equation 10, i_{e2} is the current density associated with hydrogen evolution and the last term on the right handside corresponds to the flux of H^+ from the organic to the aqueous phase (see the equilibrium Reaction 7).

Furthermore, the equilibrium constant for the second dissociation of H_2SO_4 is defined by

$$K = \frac{\left(\frac{\gamma_{H^+} \gamma_{SO_4^{2-}}}{\gamma_{HSO_4^-}} \right) \frac{(H^+)(SO_4^{2-})}{(HSO_4^-)}}{R\gamma} \quad (11)$$

where γ denote activity coefficients.

The "sulphate" mass balance is written

$$(H_2SO_4)_0 = (HSO_4^-) + (SO_4^{2-}) \quad (12)$$

neglecting the contribution of SO_4^{2-} associated with cerium ions ($Ce_2(SO_4)_3$ and $Ce(SO_4)_2$ are less concentrated compared to H_2SO_4).

Combinations of Equations 11 and 12 leads to the following expression for (H^+) :

$$(H^+) = \frac{K}{R\gamma} \frac{(HSO_4^-)}{(H_2SO_4)_0 - (HSO_4^-)} \quad (13)$$

Finally, eliminating (HSO_4^-) between Equations 10 and 13 leads to a second order algebraic equation in (H^+) , whose solution allows calculation of the proton concentration at any time and the partition coefficient, m , by combining Equations 8 and 9.

2.2. Electrochemical kinetic laws

In Part I it was shown that both anodic and cathodic processes could be described as a first approximation by a simple Butler-Volmer equation including mass transfer limitations through the Nernst film model.

The corresponding current densities are then given by the following expressions:

(i) for reaction $Ce^{3+} \rightarrow Ce^{4+} + e^-$

$$\frac{i_a}{v_e F} = \left(k_0^0 C_3 \exp \left[\alpha \frac{v_e F}{RT} (E_a - E_0^0) \right] - k_0^0 C_4 \exp \left[-\beta \frac{v_e F}{RT} (E_a - E_0^0) \right] \right) \times \left(1 + \frac{k_0^0 D_4}{k_{da} D_3} \exp \left[\alpha \frac{v_e F}{RT} (E_a - E_0^0) \right] + \frac{k_0^0}{k_{da}} \exp \left[-\beta \frac{v_e F}{RT} (E_a - E_0^0) \right] \right)^{-1}$$

where α is a function of C_3 , or in dimensionless form

$$i_a^* = A(E_a) C_3^* - A(E_a) C_4^* \times \exp \left(-(\alpha + \beta) \frac{v_e F}{RT} (E_a - E_0^0) \right) \quad (14)$$

with the expression for $A(E_0)$ given by

$$A(E_a) = \frac{k_0^0 D_4}{k_{da} D_3} \exp \left[\alpha \frac{v_e F}{RT} (E_a - E_0^0) \right] \times \left(1 + \frac{k_0^0 D_4}{k_{da} D_3} \exp \left[\alpha \frac{v_e F}{RT} (E_a - E_0^0) \right] + \frac{k_0^0}{k_{da}} \exp \left[-\beta \frac{v_e F}{RT} (E_a - E_0^0) \right] \right)^{-1}$$

(ii) for reaction $Ce^{4+} + e^- \longrightarrow Ce^{3+}$

$$\begin{aligned} \frac{i_{c1}}{v_e F} = & \left(k_0^0 C_4 \exp \left[-\beta \frac{v_e F}{RT} (E_c - E_0^0) \right] \right. \\ & \left. - k_0^0 C_3 \exp \left[\alpha \frac{v_e F}{RT} (E_c - E_0^0) \right] \right) \\ & \times \left(1 + \frac{k_0^0 D_4}{k_{dc} D_3} \exp \left[\alpha \frac{v_e F}{RT} (E_c - E_0^0) \right] \right. \\ & \left. + \frac{k_0^0}{k_{dc}} \exp \left[-\beta \frac{v_e F}{RT} (E_c - E_0^0) \right] \right)^{-1} \end{aligned}$$

or

$$\begin{aligned} i_{c1}^* = & -A'(E_c)C_3^* + A'(E_c)C_4^* \\ & - \exp \left(-(\alpha + \beta) \frac{v_e F}{RT} (E_c - E_0^0) \right) \end{aligned} \quad (15)$$

with the expression for $A'(E_c)$ given by

$$\begin{aligned} A'(E_c) = & \frac{k_0^0 D_4}{k_{dc} D_3} \exp \left[\alpha \frac{v_e F}{RT} (E_c - E_0^0) \right] \\ & \times \left(1 + \frac{k_0^0 D_4}{k_{dc} D_3} \exp \left[\alpha \frac{v_e F}{RT} (E_c - E_0^0) \right] \right. \\ & \left. + \frac{k_0^0}{k_{dc}} \exp \left[-\beta \frac{v_e F}{RT} (E_c - E_0^0) \right] \right)^{-1} \end{aligned}$$

(iii) for reaction: $2H^+ + 2e^- \longrightarrow H_2$

$$i_{c2} = a \exp(-bE_c) \quad (\text{Tafel law}) \quad (16)$$

or in dimensionless form

$$i_{c2}^* = \frac{i_{c2}}{(i_{aL})_0} = f(E_c)$$

2.3. Charge balance equation

The equality of the overall anodic and cathodic operating current intensities implies that

$$I = i_a A_{ea} = (i_{c1} + i_{c2}) A_{ec}$$

or

$$i_a^* = r(i_{c1}^* + i_{c2}^*) \quad (17)$$

2.4. Method of solution

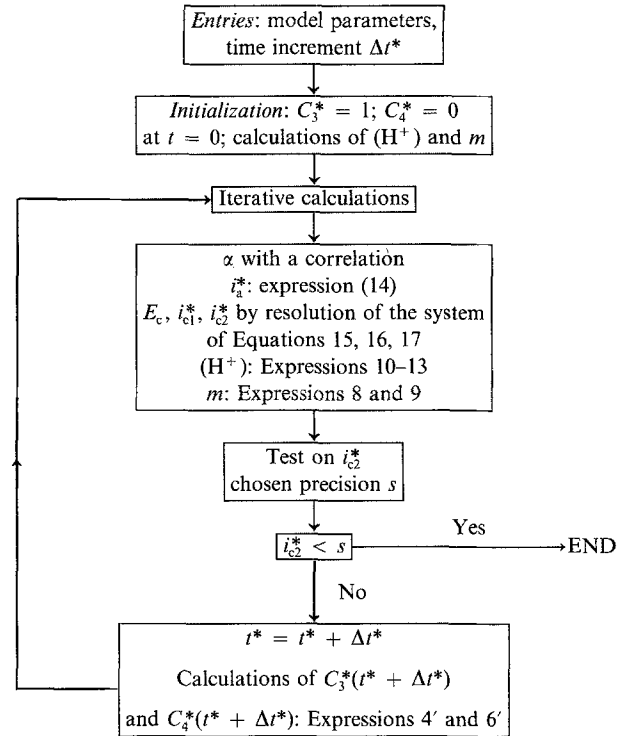
This is based on the system of differential or algebraic equations composed by Equations 2, 4, 6, 9, 13, 14, 15, 16 and 17. No analytical solution exists and a numerical integration of the system choosing an appropriate time increment Δt^* was performed for solving the differential Equations 4 and 6. Thus,

$$C_3^*(t^* + \Delta t^*) = C_3^*(t^*) - r\Delta t^* i_{c2}^*(t^*) \quad (4')$$

and

$$\begin{aligned} C_4^*(t^* + \Delta t^*) = & C_4^*(t^*) [1 - \gamma(t^*)\Delta t^*] \\ & + r\Delta t^* i_{c2}^*(t^*) \\ & - \gamma'(t^*)\Delta t^* C_3^*(t^*) + \gamma(t^*)\Delta t^* \end{aligned} \quad (6')$$

Table 1. Flowsheet of the calculations



The general flowsheet of the calculations is given in Table 1.

The final equilibrium state being defined by $i_a^* = r i_{c1}^*$ or $i_{c2}^* = 0$, a test on i_{c2}^* is used at the end of the flowsheet.

3. Validation of the model and comparison with experimental results

The validation of the model was performed by comparing the experimental and calculated time variations for:

- the Ce^{3+} and Ce^{4+} concentrations in the aqueous phase;
- the anodic current density i_a or i_a^* ;
- the partition coefficient m of cerium between the two phases.

The experiments were made potentiostatically by a procedure described in Part I of this work. The model includes different categories of parameters, which were, in some cases, taken from literature and for others determined experimentally *ex situ* and *in situ*:

- *operating parameters*: cell volume V , electrode areas A_{ea} and A_{ec} , anodic potential E_a , initial values of concentrations (Ce^{3+} , H_2SO_4 in the aqueous phase, extraction agent in the organic phase, volume ratio ε of the organic phase);
- *parameters deduced from literature*: diffusion coefficients D_3 and D_4 , equilibrium constant K , activity coefficients of H^+ , HSO_4^- and SO_4^{2-} , equilibrium potential E_0^0 , Tafel coefficients a and b for hydrogen evolution;
- *parameters determined experimentally*: mass transfer

Table 2.

| | Experiment I | Experiment II |
|--------------------------------------|--|---|
| Operation parameters | $V = 0.75 \times 10^{-3} \text{ m}^3$ $A_{\text{ea}} = 0.0734 \text{ m}^2$; $A_{\text{ec}} = 0.0496 \text{ m}^2$ $E_a = 1.78 \text{ V/NHE}$ $C_{30} = 100 \text{ mol m}^{-3}$ $(\text{H}_2\text{SO}_4)_0 = 0.5 \text{ M}$ $(\text{D}_2\text{EHPA})_0 = 800 \text{ mol m}^{-3}$ $\varepsilon = 33\%$ | $V = 0.75 \times 10^{-3} \text{ m}^3$ $A_{\text{ea}} = 0.0734 \text{ m}^2$; $A_{\text{ec}} = 0.0496 \text{ m}^2$ $E_a = 1.78 \text{ V/NHE}$ $C_{30} = 200 \text{ mol m}^{-3}$ $(\text{H}_2\text{SO}_4)_0 = 1 \text{ M}$ $(\text{D}_2\text{EHPA})_0 = 2000 \text{ mol m}^{-3}$ $\varepsilon = 33\%$ |
| Parameters deduced from literature | $D_3 = D_4 = 4 \times 10^{-10} \text{ m}^2 \text{ s}^{-1}$ $K = 0.012$ at 25°C [6] $R\gamma = 0.08$ [7] $E_0^0 = 1.44 \text{ V/NHE}$ $a = 0.1 \text{ A m}^{-2}$ $b = 230 \text{ V}^{-1}$ [8] | $D_3 = D_4 = 4 \times 10^{-10} \text{ m}^2 \text{ s}^{-1}$ $K = 0.012$ at 25°C [6] $R\gamma = 0.08$ [7] $E_0^0 = 1.44 \text{ V/NHE}$ $a = 0.1 \text{ A m}^{-2}$ $b = 230 \text{ V}^{-1}$ [8] |
| Parameters determined experimentally | $k_{\text{da}} = 3.7 \times 10^{-5} \text{ m s}^{-1}$ $k_{\text{dc}} = 2.4 \times 10^{-5} \text{ m s}^{-1}$ $k_0^0 = 3.5 \times 10^{-7} \text{ m s}^{-1}$ $\beta = 0.2$; $\alpha = 0.157 C_3^{*-0.2}$ $K_m = 2.71 \times 10^{11} (\overline{\text{HA}})_2^{-1.29}$ | $k_{\text{da}} = 3.7 \times 10^{-5} \text{ m s}^{-1}$ $k_{\text{dc}} = 1.0 \times 10^{-5} \text{ m s}^{-1}$ $k_0^0 = 3.5 \times 10^{-7} \text{ m s}^{-1}$ $\beta = 0.2$; $\alpha \approx 0.225$ $K_m = 7.07 \times 10^8 (\overline{\text{HA}})_2^{-2.26}$ |

coefficients k_{da} and k_{dc} , electrochemical kinetic parameters k_0^0 , β , α , apparent equilibrium constant K_m characterizing the extraction mechanism of Ce^{4+} . For the determination of the kinetic parameters k_0^0 , β and α , two independent procedures were used: (i) the one described in Part I of this work is based on the analysis of the current potential curves obtained *ex situ* on a platinized titanium plate in a laboratory cell or on a platinum 3 mm rotating disc electrode using different Ce^{3+} concentrations. (It should be remembered that α depends slightly on the bulk concentration of Ce^{3+} due to the formation of complex compounds between Ce^{3+} and SO_4^{2-} ions — see, for example, Fig. 3 in Part I). From this first procedure, the values of k_0^0 , β and α may be deduced, and (ii) the second procedure is based on the analysis of the experimental relation between i_a and C_3 (or i_a^* and C_3^*) determined *in-situ* during the potentiostatic experiments. Indeed, for high anodic electrode potentials, E_a , Equation 14 reduces to $i_a^* = A(E_a)C_3^*$.

Consequently, the experimental time variations of i_a^* and C_3^* are used to calculate $A(E_a)$ and then α and to deduce an adequate correlation between α and C_3^* .

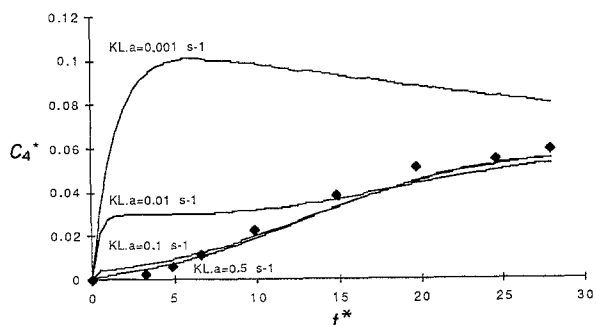


Fig. 1. Influence of the overall liquid-liquid mass transfer coefficient k_{La} on the calculated time-variation of C_4^* (see Table 2). (◆) Comparison with the results of experiment I.

Within experimental precision both procedures lead to the same values of α [5].

With regards to the equilibrium constant, K_m , its determination and the obtaining of the corresponding correlation between K_m and $(\overline{\text{HA}})_2$ were based on the analysis of the experimental time-variations of Ce^{3+} and Ce^{4+} by calculating at any time \overline{C}_4 , m , H^+ , $(\overline{\text{HA}})_2$ and finally K_m with Equation 8.

K_m , which depends on the concentration of the dimer form $(\overline{\text{HA}})_2$ of the extraction agent as discussed in Part I of this work, therefore appears as an adjustable parameter in the model.

A comparison between the experimental results and the model predictions was made for two sets of experiments, whose operating conditions are given in Table 2. It should be noted that the two experiments largely differ by the initial values of the concentrations C_{30} , $(\text{H}_2\text{SO}_4)_0$ and $(\text{D}_2\text{EHPA})_0$; it is therefore not surprising that the correlations obtained for α and K_m are different given the importance of the formation of complex compounds.

For the operating conditions of experiment I, Fig. 1 presents the influence of the overall liquid/liquid mass transfer coefficient k_{La} (which was difficult to determine

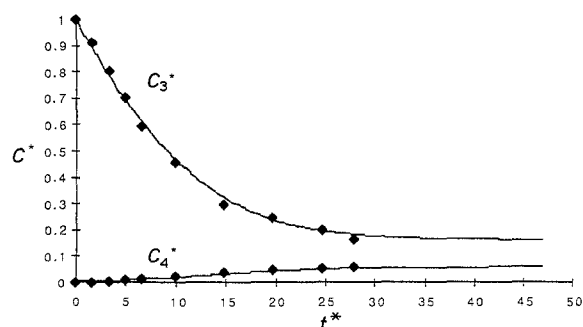


Fig. 2. Calculated time-variations (full line) of C_3^* and C_4^* for the conditions of experiment I (see Table 2). (◆) Comparison with the experimental results.

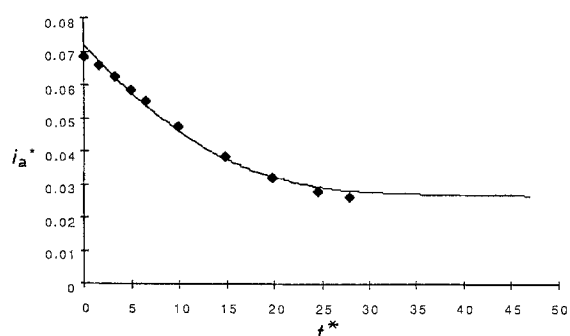


Fig. 3. Calculated time variations (full line) of the dimensionless anodic current density i_a^* (conditions of experiment I) (see Table 2). (◆) Comparison with the experimental results.

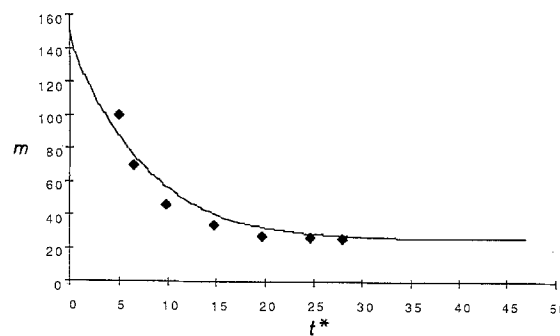


Fig. 4. Calculated time-variations (full line) of the partition coefficient m (conditions of experiment I) (see Table 2). (◆) Comparison with the experimental results.

experimentally) on the calculated time-variations of C_4^* ; for small value of k_{La} (for example 10^{-3} s^{-1}), i.e. a low extraction rate, the curve is characterized by the existence of a maximum which can be explained by the high concentration of Ce^{4+} attainable in the aqueous phase and consequently the possible importance of the cathodic consumption flux. However as k_{La} increases, the extraction rate becomes sufficient for maintaining a low Ce^{4+} concentration in the aqueous phase and minimizing its cathodic reduction. It should be noted that the experimental results plotted in the same figure clearly show that the extraction of Ce^{4+} by the organic phase is not rate-determining; the value $k_{La} = 0.1 \text{ s}^{-1}$ for which the curve C_4^* against t^* has reached its limiting position, was therefore chosen for the model calculations.

The curves 2, 3, 4 for experiment I and 5, 6, 7 for

experiment II compare the calculated time-variations of C_3^* and C_4^* in the aqueous phase (Figs 2 and 5), the anodic current densities i_a^* (Figs 3 and 6) and of the partition coefficient m (Figs 4 and 7) to the experimental values. For the two sets of experiments (and others not present here) the agreement is satisfactory which confirms the present model and its hypotheses.

4. Conclusion

A simple model able to predict the transient behaviour of a batch undivided electrochemical reactor operated potentiostatically with simultaneous *in situ* extraction of the product by an organic phase has been successfully evolved.

For the particular case of the $\text{Ce}^{3+}/\text{Ce}^{4+}$ system, all the model parameters (mainly electrochemical kinetic

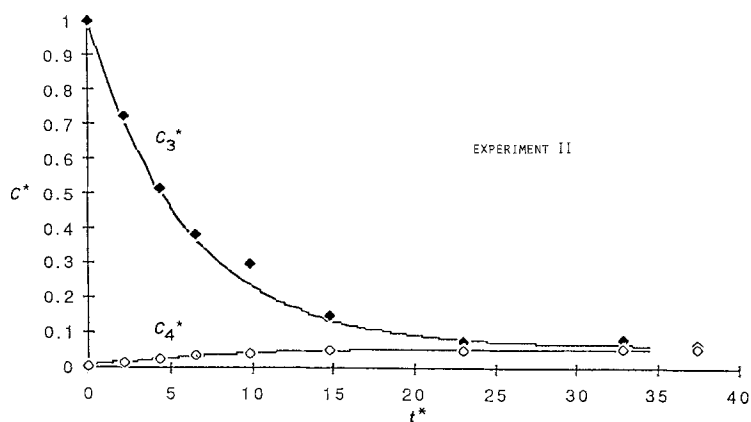


Fig. 5. Calculated time variations (full line) of C_3^* and C_4^* for the conditions of experiment II (see Table 2). (◆) and (◇) Comparison with the experimental results, respectively.

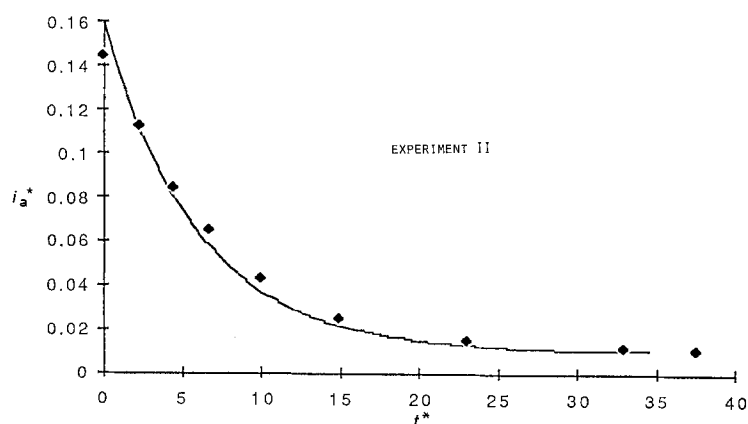


Fig. 6. Calculated time-variations (full line) of the dimensionless anodic current density i_a^* (conditions of experiment II) (see Table 2). (◆) Comparison with the experimental results.

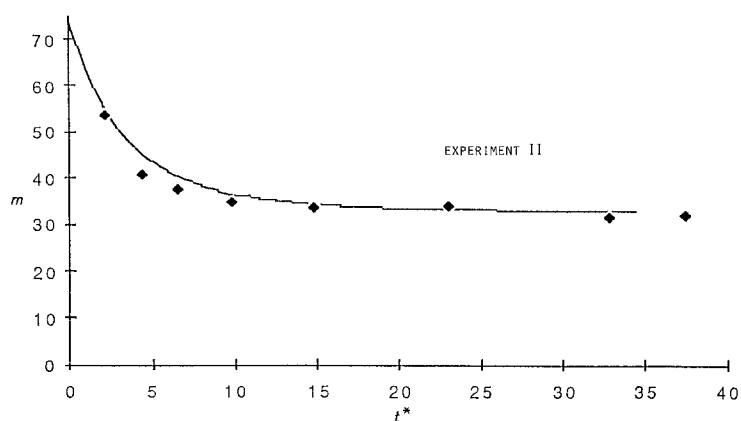


Fig. 7. Calculated time-variations (full line) of the partition coefficient m (conditions of experiment II) (see Table 2). (◆) Comparison with the experimental results.

parameters, liquid-solid mass transfer coefficients, liquid-liquid equilibrium constant) may be determined independently by *ex situ* measurements.

The predictions of the model are found to be in very good agreement with the experimental results for a large range of concentrations of cerium, sulphuric acid and extraction agent.

References

- [1] D Horbez and A. Storck, *J. Appl. Electrochem.* this issue.
- [2] A. Storck and F. Coeuret, 'Éléments de Génie Electrochimique, Technique et Documentation', Lavoisier, Paris (1984).
- [3] T. Z. Fahidy, 'Principles of Electrochemical Reactor Analysis', Elsevier, Amsterdam (1985).
- [4] E. Heitz and G. Kreysa, 'Principles of Electrochemical Engineering', VCH, Weinheim (1986).
- [5] D. Horbez, Thèse, Institut National Polytechnique de Lorraine (Septembre 1988).
- [6] CRC 'Handbook of Chemistry and Physics', 67th edition, CRC Press (1987).
- [7] 'Gmelins Handbuch der Anorganischen Chemie', Teil B2 Schwefel (1960) 748-53.
- [8] Y. Lourie, Aide-mémoire de Chimie Analytique, edition Masson, Paris (1975).